Stiffness Regulates the Morphology and Stemness of Limbal Niche Cells Through Unique nYAP/cYAP Translocation

Xiao Zhou, Lingjuan Xu, Yongyao Tan, Wei Wang, Xiaoyu Huang, and Guigang Li

Department of Ophthalmology, Tongji Hospital, Tongji Medical College, Huazhong University of Science and Technology, Hubei Key Laboratory of Otolaryngologic and Ophthalmic Diseases, Wuhan, China

Correspondence: Guigang Li, Department of Ophthalmology, Tongji Hospital, Tongji Medical College, Huazhong University of Science and Technology, 1095 Jiefang Rd., QiaoKou District, Wuhan 430030, China; guigangli@hust.edu.cn.

XZ, LX, and YT contributed equally to the work presented here and should therefore be regarded as equivalent authors.

Received: November 9, 2024
Accepted: January 23, 2025
Published: February 14, 2025

Citation: Zhou X, Xu L, Tan Y, Wang W, Huang X, Li G. Stiffness regulates the morphology and stemness of limbal niche cells through unique nYAP/cYAP translocation. *Invest Ophthalmol Vis Sci.* 2025;66(2):43. https://doi.org/10.1167/iovs.66.2.43

Purpose. To investigate the effect of matrix stiffness on the morphology and stem characters of maintenance and differentiation of limbal niche cells (LNCs) and the mechanisms involved.

Methods. Human LNCs were isolated, cultured, and identified based on published literature, and LNCs from passages 4 to 6 (P4–P6) were used in this study. They were coated with hydrogels of different concentrations to prepare matrices with different stiffnesses, and non-coated plate were used for the control group. Elastic modulus values were determined by atomic force microscopy (AFM). The expression of putative stem cell markers (SOX2, OCT4, PAX6) and fibrosis markers (α-SMA, COL1A1, S100A4) was analyzed by immunofluorescence and quantitative reverse-transcription PCR (RT-qPCR). The intracellular distribution and expression of Yes-associated protein (YAP) and drosophila mothers against decapentaplegic protein family members 2 and 3 (SMAD2/3) accordingly were analyzed using immunofluorescence and western blot.

Results. The elastic modulus values of plastic, low-concentration hydrogel–coated surfaces, and high-concentration hydrogel–coated surfaces were 3261.05 $\pm$ 172.78 MPa, 30.39 $\pm$ 5.84 kPa, and 6.99 $\pm$ 4.04 kPa, respectively; thus, they were referred to as the dish, stiff, and soft groups. Using an in vitro model to explore the effect of matrix stiffness on LNCs, we found that a soft substrate could activate YAP to change the morphology and elevate the stemness of LNCs, whereas activation of SMAD2/3 on a stiff substrate decreased nuclear YAP (nYAP) levels, leading to myofibroblast phenotype. Inhibition of SMAD2/3 on stiff substrates partially restored LNC stemness by promoting YAP nuclear translocation.

Conclusions. Our findings confirm that matrix stiffness regulates the stemness and differentiation of LNCs through the YAP/SMAD signaling pathway, indicating a potential strategy for the treatment of limbal stem cell deficiency based on LNCs.

Keywords: LNCs, substrate stiffness, stemness, YAP, SMAD2/3

Limbal niche cells (LNCs) are located in the limbal region of the eye, the boundary between the cornea and sclera. This region harbors a special microenvironment (known as the limbal niche) that maintains the integrity and function of the corneal epithelium by supporting limbal stem cells (LSCs).[1–3] In previous studies, LNCs have been shown to express vimentin and embryonic stem cell markers such as octamer-binding transcription factor 4 (OCT4) and SRY-box transcription factor 2 (SOX2),[4,5] and they have the ability to induce mature corneal epithelial cells (MCECs) to de-differentiate into LSCs.[6,7] However, subjecting LNCs to serial passages on rigid plastic has led to irreversible reprogramming of the myofibroblast phenotype,[8] highlighting the impact of the mechanical environment on cell behavior. Essentially, the biomechanical rigidity of the human limbal niche is lower compared to that of the differentiated zone,[9] and it has been demonstrated that a rigid matrix can induce LSC differentiation.[10]

Yes-associated protein (YAP) is expressed in various tissues of mammals,[11] and its expression status is considered to be highly correlated with the rigidity of the surrounding matrix.[12–14] Interestingly, the effect of substrate stiffness on the subcellular distribution of YAP remains controversial. Some studies have reported that YAP transfers from the cytoplasm (cYAP) to the nucleus (nYAP) in response to a perceived stiff substrate, thereby activating a mechanistic response pathway that promotes stem cell proliferation and differentiation.[13,15–19] However, the nuclear translocation of YAP (nYAP) to maintain the undifferentiated state of stem cells in soft substrate has also been observed by other researchers.[20–22] Our previous study found that LNCs can effectively maintain the undifferentiated phenotype of limbal epithelial stem cells in a three-dimensional (3D) environment composed of soft matrix, as demonstrated by larger spheroids, higher levels of the stem cell marker P63α, and lower levels of the differ-

entiation marker CK12.[6] The drosophila mothers against decapentaplegic protein (SMAD) family proteins have been proven to play a crucial role in the TGF-β signaling pathway.[23] Typically, active phosphorylated SMAD2/3 proteins translocate to the nucleus to regulate multiple cellular processes, such as cell proliferation, apoptosis, and differentiation. Recent studies have indicated that SMAD2/3 proteins can also respond to mechanical signals, leading to cell differentiation, and can crosstalk with the YAP pathway.[24–26] Therefore, we propose that YAP and SMAD2/3 may have a unique mechanism and regulatory network in the cornea.

In the current study, we investigated the nYAP/cYAP translocation mechanism in LNCs by adjusting substrates stiffness during cell culture. We conducted a comprehensive investigation of LNC morphology, stem cell characteristics, and YAP expression to evaluate the impact of this mechanism on LNC behavior. These findings may offer important insights into the mechanisms of fibrosis and provide new strategies for the treatment of corneal and ocular surface diseases.

Materials and Methods

Preparation of Substrates of Varying Stiffness

Hydrogels with different levels of stiffness were prepared by adjusting the chemical composition of polyacrylamide (PA) solution. Both 40% w/v acrylamide (Sangon Biotech, Shanghai, China) and 2% w/v methylenebisacrylamide (Sangon Biotech) were sterilized by filtration through 0.2-µm disposable pinhead filters. Acrylamide and methylenebisacrylamide of the required composition (Table) were mixed to a final volume of 10 mL. To initiate polymerization, 1/100 of the total volume of ammonium persulfate (APS) (Sinopharm Group, Shanghai, China) and 1/1000 of the total volume of tetramethylethylenediamine (TEMED) (Klamar, Shanghai, China) were added to the acrylamide–methylenebisacrylamide mixture.

Stiffness Measurement by Atomic Force Microscopy

The stiffness of the hydrogel was determined by atomic force microscopy (AFM; Bruker, Billerica, MA, USA) in contact mode. Carefully remove the hydrogel after solidification, the sample was immersed in a 1× PBS liquid environment and measured using a spherical AFM tip probe with a radius of about 5 µm to minimize the strain field. Seven points on each sample were randomly selected and measured, and each substrate was randomly measured three times.[27] The results were analyzed using Atomic Force Microscope operating software (Asylum Research, Santa Barbara, CA, USA). Stiffness is expressed as the mean ± SD.

Table. Related Components of Polyacrylamide Hydrogels With Different Stiffness

	Soft Substrate (mL)	Stiff Substrate (mL)
40% Acrylamide	0.75	2
2% Methylenebisacrylamide	1.5	1.32
ddH_2O	7.75	6.68

ddH_2O, double-distilled water.

Isolation and Culture of LNCs

Healthy donor corneas between 50 and 70 years old were obtained from the Red Cross Eye Bank of Wuhan Tongji Hospital (Hubei, China) and managed in accordance with the tenets of the Declaration of Helsinki. All experiments were approved by the Ethics Committee of Tongji Hospital (TJ-IRB20230899). Supplementary Table S1 provides records of the donors.

Human LNCs were isolated and cultured as described previously.[4,28] Following the standard operating procedures of the eye bank, we removed the donor corneal ring and placed it in the medium-term solution (Eusol-C; Alchimia srl, Ponte San Nicolò, Italy). Several days later (no more than 5 days generally), we removed the corneal limbal tissue from the corneal storage medium. Working within a sterile environment, we used 2 mg/mL collagenase A to digest limbal explants at 37°C for 16 hours to produce clusters containing the entire limbal epithelium and underlying stromal cells. The clusters were further digested at 37°C with 0.25% trypsin/0.5-mM EDTA (TE) for 15 minutes to obtain single cells and were then inoculated into six-well plates coated with 5% Matrigel at a density of $1 \times 10^5/cm^2$ in modified embryonic stem cell medium (MESCM). Detailed information on the composition and concentration of the MESCM can be found in Supplementary Table S2. After the cell density reached 80% to 90%, LNCs were passed continuously at a density of $1 \times 10^5/cm^2$. P4 to P6 LNCs were used for follow-up experiments when cultured in substrates with different stiffnesses. After 10 days of incubation, samples from the different groups were photographed and subjected to immunocytochemistry, western blot, and quantitative reverse-transcription PCR (RT-qPCR) analyses. In subsequent experiments, we examined the expression of SMAD2/3 on day 5 of culture. All materials used for cell isolation and culture are listed in Supplementary Table S2.

Hematoxylin and Eosin Staining

Human eye samples were fixed and then paraffin embedded and sliced. Paraffin sections were dewaxed to water. After the three cylinders of xylene were used to dehydrate for 10 minutes each, the gradient alcohol (100%, 95%, 75%) was hydrated for 5 minutes per cylinder. After washing with pure water, EDTA (pH 9.0) was used for antigen repair. After the repair solution was cooled to room temperature, we removed the slices and soaked them in pure water for 3 minutes.

Hematoxylin staining solution was then applied for 4 minutes followed by washing under tap water for 2 minutes. Then, 1% hydrochloric acid alcohol was differentiated for 3 seconds, followed by rinsing with tap water and subsequent examination under a microscope to assess the staining intensity. Eishin dye solution was used for 20 seconds, and the water washing step was bypassed, instead proceeding directly to gradient alcohol dehydration (80%, 90%, 95%, and 100%), use xylene to transparent, sealing, and microscopic examination.

Immunocytochemistry and Immunohistochemistry

TE was applied to digest the adherent LNCs into a suspended state. Then, a StatSpin CytoFuge2 (Beckman Coulter, Brea, CA, USA) was used to prepare cell smears at 1000 rpm for

Investigative Ophthalmology & Visual Science

4 minutes at a cell density of 1×10^4 per slide for immunofluorescence staining. After air drying for 5 minutes, the cell smear was fixed with 4% paraformaldehyde for 15 minutes, permeated with 0.3% Triton X-100 on PBS for 12 minutes, sealed with 10% donkey serum for 1 hour, and then incubated with primary antibody at 4°C overnight. The second antibody was detected by incubating at room temperature for 2 hours and restaining the nucleus with DAPI. Paraffin sections were dewaxed to water as above, and antigenic repair was performed. The following steps were the same as for cellular immunofluorescence. The results were observed using a confocal laser scanning microscope (LSM700; Carl Zeiss Microscopy, Jena, Germany) and photographed using NIS-Elements software (Nikon, Tokyo, Japan). Detailed information regarding the primary and secondary antibodies and other reagents is provided in Supplementary Table S3.

Western Blotting Analysis

LNCs were lysed in radioimmunoprecipitation assay (RIPA) cleavage and extraction buffer containing 1% phenylmethylsulfonyl fluoride protease inhibitor. The nuclear and cytoplasmic components of YAP were dissociated by NE-PER Nuclear and Cytoplasmic Extraction Reagents (78833; Thermo Fisher Scientific, Waltham, MA, USA). Protein concentrations were measured by a bicinchoninic acid (BCA) protein assay kit (23225; Thermo Fisher Scientific). The proteins were blocked with 5% milk for 1 hour at room temperature. The list of antibodies is provided in Supplementary Table S3. Finally, protein bands were detected by chemiluminescence using electrochemical luminescence reagents. The staining intensity was quantified using ImageJ (National Institutes of Health, Bethesda, MD, USA).

RNA Extraction and RT-qPCR

Total RNA was isolated using Invitrogen TRIzol (Thermo Fisher Scientific) and purified according to the manufacturer's protocol. A NanoDrop microspectrophotometer (Thermo Fisher Scientific) was used to determine the absorption value of RNA solutions at 260 nm to calculate RNA concentration and purity. Reverse transcription of cDNA using a high-volume kit (Applied Biosystems, Foster City, CA, USA) and ChamQ Universal SYBR qPCR Master Mix (Vazyme, Nanjing, China) was used to detect target genes. Data were standardized using an internal control glyceraldehyde-3 phosphate dehydrogenase. For each primer group, all assays were performed in triplicate. The standard $2^{-\Delta\Delta Ct}$ method was used to quantify relative gene expression. The primer sequence is provided in Supplementary Table S4.

Animal Model of Limbal Stem Cell Deficiency

Male or female Bal/BC mice (n =3) were kept in captivity under pathogen-free conditions and fed a standard diet. Adult mice 6 to 8 weeks old were anesthetized by intraperitoneal injection of 100 mg/kg ketamine and 10 µg/g toluene thiazide. A filter paper immersed in 1-M sodium hydroxide (NaOH) was attached to the right cornea of the mouse right eye for 30 seconds, and then the eye was rinsed with 0.9% sodium chloride (NaCl) to induce limbal stem cell deficiency (LSCD).[29] The uninjured left eye served as a control. Then, 15 days after the alkali burn, the mouse was euthanized and samples were collected.

Statistical Analysis

Statistical analysis was performed using Prism 9.0 (GraphPad, Boston, MA, USA). The data in this study followed a normal distribution and thus are expressed as the mean ± SD of independent experiments. Differences among normally distributed values of the three experimental groups were analyzed by one-way ANOVA with Tukey's correction for multiple comparisons. All measurements were made in triplicate. $P < 0.05$ was considered statistically significant.

Results

Isolation and Culture of LNCs

As shown in Figure 1A, limbus located at the annular zone marked the tissue boundary between the cornea and adjacent sclera. In contrast, differentiated cells, referred to as MCECs, were situated in the central cornea, which is microscopically distinguishable. The anatomically similar LSCs and LNCs were closely adjacent to each other and located in the palisade of Vogt of the limbal microenvironment (Supplementary Fig. S1). To isolate clusters containing LNCs, we minced corneoscleral rings into 16 equal pieces, and then the small pieces were digested with collagenase A (Fig. 1B). After that, LNCs were seeded on coated Matrigel and cultured for 10 days in MESCM. Consistent with our previous study, P0 cells were a mixture of pancytokeratin $(PCK)^+$/vimentin $(Vim)^-$ epithelial cells and PCK^-/Vim^+ mesenchymal cells, whereas P4 LNCs were uniformly PCK^-/Vim^+ cells. Briefly, we purified LNCs as described earlier in the discussion regarding purification of the MESCM (Fig. 1C).

Substrate Stiffness Affected LNC Morphology

Previous measurements of corneal stiffness in humans have shown that the human central cornea (20 kPa) is much stiffer than the limbus (8 kPa).[30] Using an in vitro model, we developed a strategy to investigate the response of LNCs to different stiffnesses. Specifically, we constructed PA gels of varying stiffness (stiff or soft) and used direct culture on plastic plates as a control (referred to here as dish). The Young's modulus values as measured by AFM for stiff and soft substrates were 30.39 ± 5.84 kPa and 6.99 ± 4.04 kPa, respectively (Fig. 1D). These values are close to the stiffness values of the central cornea and limbus,[20] whereas the plastic surface stiffness was 3261.05 ± 172.78 MPa. Because the limbus extracellular matrix serves as the stem cell niche, its stiffness may play an important role in LNC regulation.

P4 LNCs were grown on different surfaces and photographed at day 1 (D1), day 5 (D5), and day 10 (D10). At D1, LNCs were attached to all substrates with significant morphological diversity. In the dish group and the stiff group, LNCs grew in a spindle shape, and the stiff group grew better than the dish group. However, in the soft group, LNCs were smaller and tended to form spheres (Fig. 2). These results suggest that substrate stiffness can affect the morphology of LNCs, which were smaller and rounder on the soft substrate.

Investigative Ophthalmology & Visual Science

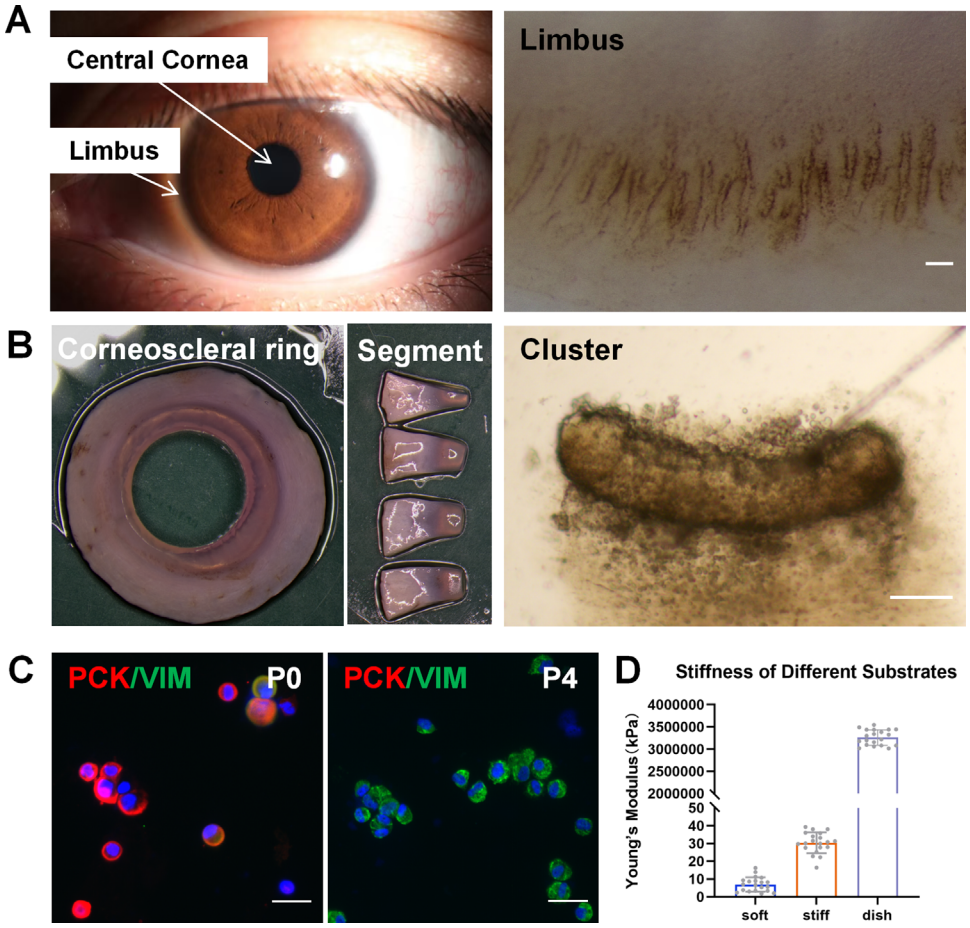

Figure 1. Isolation and culture of human LNCs. (**A**) Image of human eye and limbus. *Scale bar*: 200 µm. (**B**) Corneoscleral rings. After 16 hours of collagenase digestion, clusters of cells isolated from the limbus were visible. *Scale bar*: 200 µm. (**C**) After TE digestion, a large number of PCK^+ epithelial cells and a small number of Vim^+ LNCs were observed in P0 cells. At P4, the cells expressed Vim uniformly, suggesting that epithelium was removed from the LNCs. *Scale bar*: 100 µm. (**D**) Hydrogels of varying stiffness. The elastic moduli of the soft, stiff, and dish groups were calculated using AFM from three independent experiments. Indentation points = 7 for each experiment. All quantitative data are presented as mean ± SD.

Soft Substrates Enhanced the Stemness of LNC

Given the altered morphology, we determined whether or not LNCs were altered in the phenotype of the embryonic stem cells. Representative stemness markers (SOX2, OCT4) and the eye development marker (paired box 6 [PAX6]) were selected. As shown in Figure 3A, a large number of positive cells were observed in groups with the soft PA gel, whereas the opposite trend was observed in the dish group. Also, there was a significant difference observed between the dish and stiff groups. We then investigated whether the stemness and eye development in LNCs belonging to different groups showed differences in their transcription levels. RT-qPCR assays showed that SOX2, OCT4, and PAX6 transcription levels were increased in the soft group (Fig. 3B). These results suggest a stimulated effect of soft substrates on LNC stemness in vitro.

Rigid Substrates Confer LNC Myofibroblast Phenotype

Although we showed that a soft substrate enhanced stemness expression in LNCs, it was not clear whether the regulation effect works in other processes in LNCs. We found that the morphological changes did not reveal the phenotype switch of the mesenchymal stem cells (MSCs) (Supplementary Fig. S2). However, immunofluorescence results showed that LNCs that have expanded on plastic and stiff substrates acquire characteristics of myofibroblasts, α-smooth muscle actin (α-SMA) and S100A4, and secreted collagen 1 (COL-1) (Fig. 4A). In contrast, this phenomenon did not occur in the soft group. Subsequently, we validated the results of the immunofluorescence analysis using RT-qPCR (Fig. 4B). Interestingly, levels of laminin, an important component of basement membranes, were increased in the soft group (Supplementary Fig. S3). Our results revealed that rigid substrates initiated fibrotic progress in LNC.

Substrates Stiffness Regulated YAP Localization

Immunofluorescence images showed localization and expression of YAP in the different groups. Compared with LNCs in the dish and stiff groups, LNCs cultured on soft substrates showed higher YAP expression levels and greater nuclear localization of YAP (Fig. 5A, Supplementary Fig. S4). As shown in Figure 5B, the use of a nuclear and cytoplasmic

Investigative Ophthalmology & Visual Science

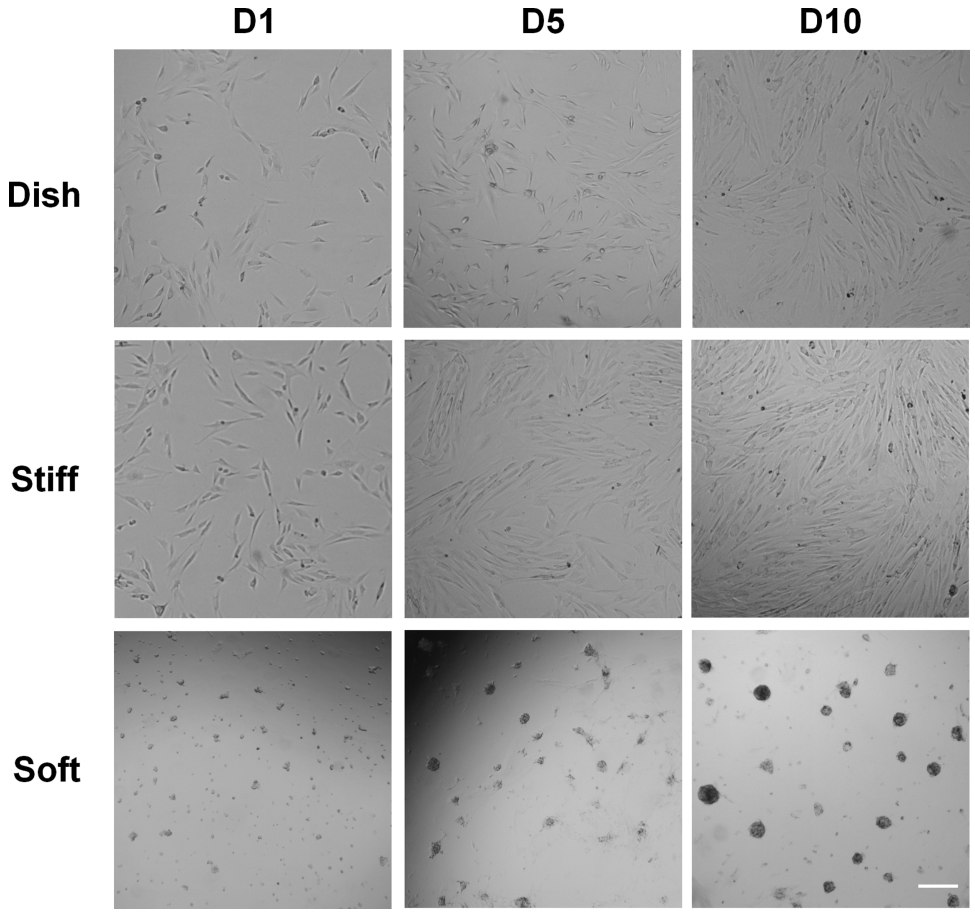

Figure 2. LNCs were cultured on hydrogels of varying stiffness. There were significant differences in cell morphology. In the dish and stiff groups, the LNCs grew in a spindle shape, whereas, in the soft group, the cells were smaller and rounder and had a tendency to aggregate into spheres. *Scale bar*: 200 µm.

extraction kit revealed that there was a significant increase of nuclear YAP in the soft group, and the expression levels of total YAP were also elevated (Fig. 5C). Such results suggest that substrate stiffness largely affects YAP nuclear accumulation, but it is not known how.

Next, the expression pattern of YAP in mouse limbus was characterized by YAP immunohistochemical staining. YAP was predominantly and consistently expressed in the nuclear form within the limbus region. However, in a mouse model of alkali burn, YAP exhibited characteristics of cytoplasmic expression (Fig. 6A). The expression of YAP in the cornea of mice and alkali-burned mice is shown in Supplementary Figure S4. The detection of nYAP in the limbus region and the loss of YAP nuclear localization in alkali-burned mice indicate that YAP plays a broad role in LNCs.

Blocking of SMAD2/3 in LNC Reversed Phenotype Switching

Our results are not consistent with many studies linking nYAP to stiffer substrates; however, other studies have recently reported that softer substrates enhance nYAP in stem cells. Bhattacharya et al.[20] proposed that the reason may be that the stiffness of the cornea compared with other tissues stimulates another signaling pathway in effect before the YAP–SMAD signaling pathway, leading to cYAP localization. After a search of the STRING website, we used Cytoscape software to draw a protein interaction map that shows significant crosstalk between YAP and SMAD proteins, including SMAD2 and SMAD3 (Fig. 6B). Therefore, we examined SMAD2/3 expression in LNCs grown for 5 days on substrates of varying stiffness. Significant nuclear SMAD2/3 was detected on substrate of corneal stiffness (stiff group), whereas in the soft group, SMAD2/3 was mostly expressed in the cytoplasm (Fig. 7A). Together, these data suggest that substrate stiffness affects YAP localization and expression in LNCs and is associated with the SMAD pathway.

Extracellular matrix (ECM) stiffness controlled the subcellular localization of SMAD2/3, and this change was earlier and stronger than that of YAP. To further verify the involvement of SMAD2/3 in stiffness regulation of LNC morphology and stemness, SMAD2/3 inhibitor SB431542 and YAP inhibitor verteporfin were used in subsequent experiments. We found that SB431542 inhibited the reduction in corneal stiffness of nuclear SMAD2/3 (Fig. 7A). Importantly, SB431542 treatment also promoted YAP nuclear translocation, suggesting that SMAD2/3 negatively regulates YAP expression.

Western blot results also showed that the levels of stiff group SMAD2/3 and phosphorylated SMAD2/3 (p-SMAD2/3) were significantly higher, and it was shown

Investigative Ophthalmology & Visual Science

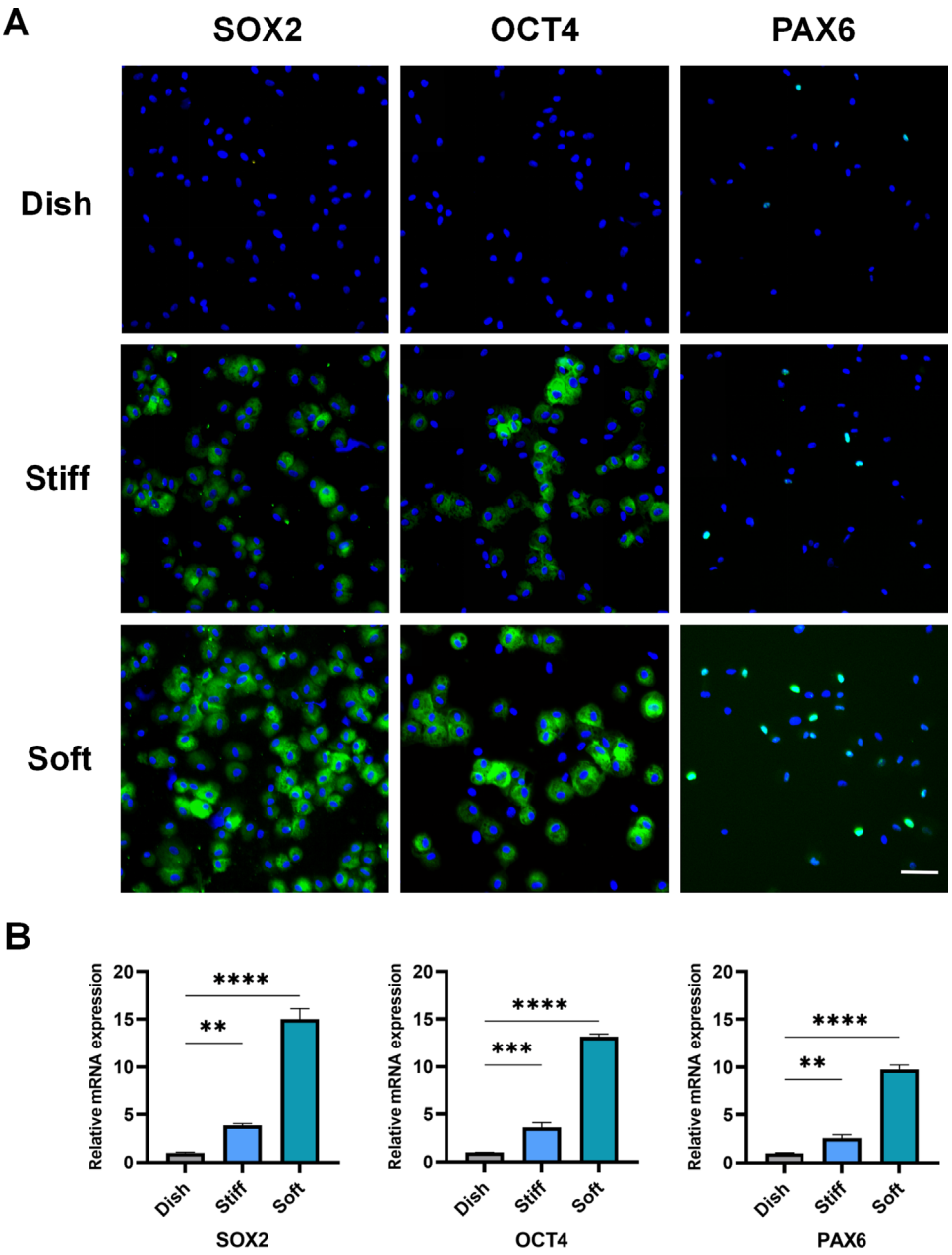

Figure 3. Expression of embryonic stem cell markers in LNCs cultured with hydrogels of different stiffness after 10-day culture. (**A**) Immunostaining of SOX2, OCT4, and PAX6 of LNCs on dish, stiff, and soft substrates. *Scale bar*: 200 µm. (**B**) The mRNA expression of SOX2, OCT4, and PAX6 of LNCs on dish, stiff, and soft substrates after 10-day culture. All quantitative data are presented as mean ± SD. ****$P < 0.0001$, ***$P < 0.001$, **$P < 0.01$.

that p-SMAD2/3 enters the nucleus to function. After using the SMAD inhibitor SB431542, the expression of p-SMAD2/3 was suppressed. Furthermore, we found that, upon addition of SB431542 to the stiff group, the expression of stem cell markers SOX2, OCT4, and PAX6 was partially restored. Conversely, when the YAP inhibitor verteporfin was added to the soft group, the stem cell characteristics of LNCs were decreased (Supplementary Fig. S5).

These findings allowed us to propose a novel mechanistic model elucidating how matrix stiffness modulates the behavior and phenotype of LNCs. In this model, the softer characteristics of the limbus facilitate the translocation of YAP into the nucleus, thereby sustaining the undifferentiated state of stem cells and maintaining elevated expression levels of SOX2, OCT4, and PAX6. Conversely, with regard to corneal stiffness, an alternative pathway involving SMAD2/3 is activated to enter the nucleus, inhibiting the nuclear entry of YAP and promoting cellular differentiation (Fig. 8).

Discussion

Scarring of the cornea and other ocular surface tissues is one of the main symptoms of LSCD.[31,32] In the process of scar progression, abnormal precipitation of the ECM, such as COL-1, will lead to changes in the matrix compo-

Investigative Ophthalmology & Visual Science

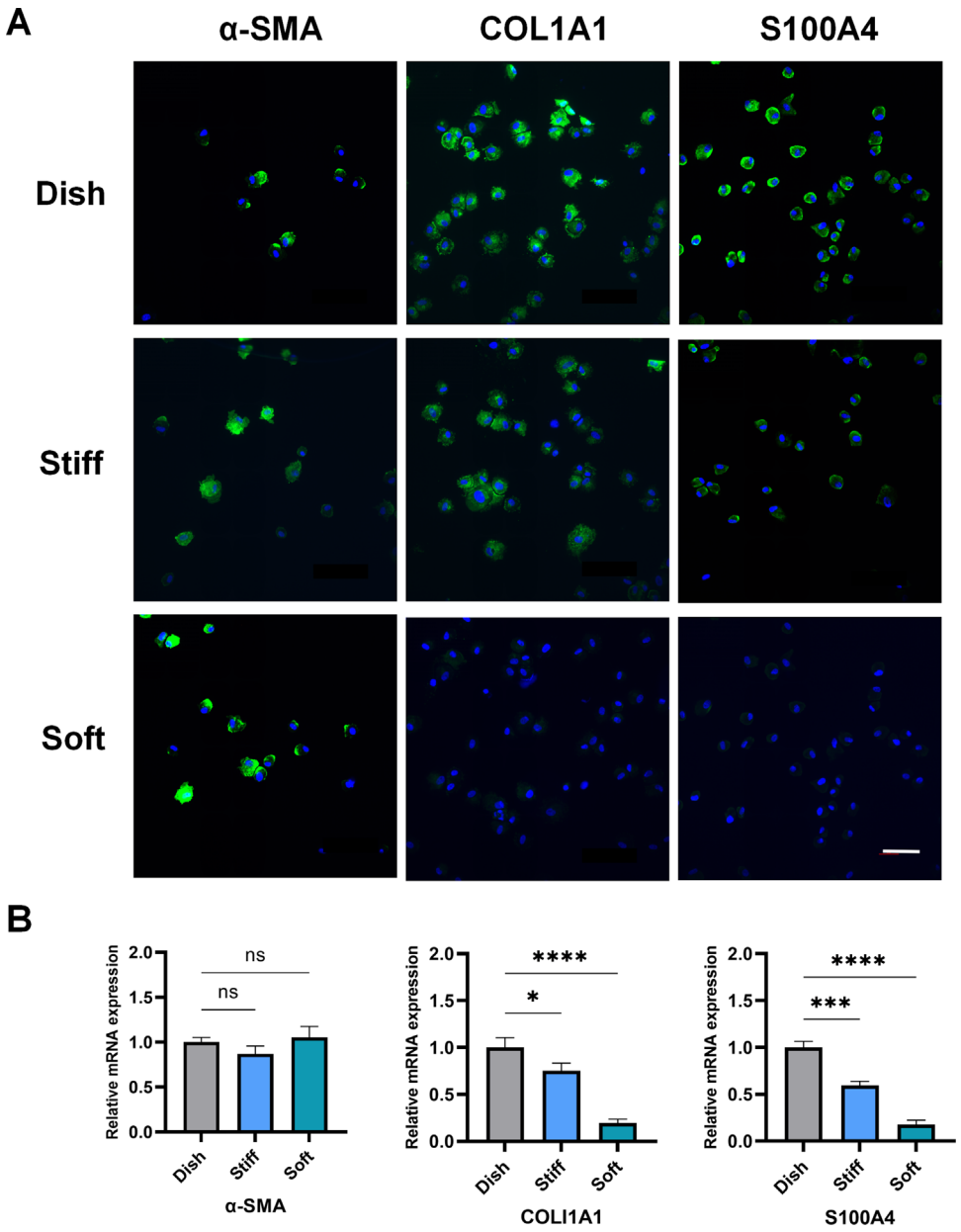

Figure 4. Expression of fibrosis markers in LNCs cultured with hydrogels of different stiffness. (**A**) Immunostaining of α-SMA, COL1A1, and S100A4 of LNCs on dish, stiff, and soft substrates after 10-day culture. *Scale bar*: 200 µm. (**B**) The mRNA expression of α-SMA, COL1A1, and S100A4 of LNCs on dish, stiff, and soft substrates after 10-day culture. All quantitative data are presented as mean ± SD. ****$P < 0.0001$, ***$P < 0.001$, *$P < 0.05$.

sition of the limbal niche; that is, the matrix stiffness increases.[33] Basically, a softer or more physiologically appropriate matrix stiffness would favor the maintenance of of stem cell pools,[34,35] and this theory could also explain the behavior of LSCs with regard to the central corneal and limbal stiffness. Our previous studies have shown that LNCs are an important part of the limbal niche and can maintain the undifferention and function of LSCs. Interestingly, continuous passage of LNCs on rigid plastic is subject to irreversible reprogramming of myoblast phenotypes, which is not seen in 3D soft environments for the same components.[8]

In order to study the effect of matrix stiffness on LNCs, we established PA gel-based culture systems with varying stiffness. Not surprisingly, LNCs first exhibited different growth morphologies in cultures with different stiffness. Specifically, the LNCs maintained a consistent spindle shape in the dish and stiff groups but grew spherically in the soft group. However, the morphological changes did not reveal the phenotype of MSC (Supplementary Fig. S2), but instead affected the embryonic stem cell phenotype, and there was a definite decline in PAX6 (Fig. 3), which represents the phenotype of the neural crest and eye development.

In addition, although the LNCs in the stiff group retained the characteristics of MSCs, they again showed a transformation toward the myofibroblast phenotype, as evidenced by positive levels of α-SMA and S100A4, whereas the posi-

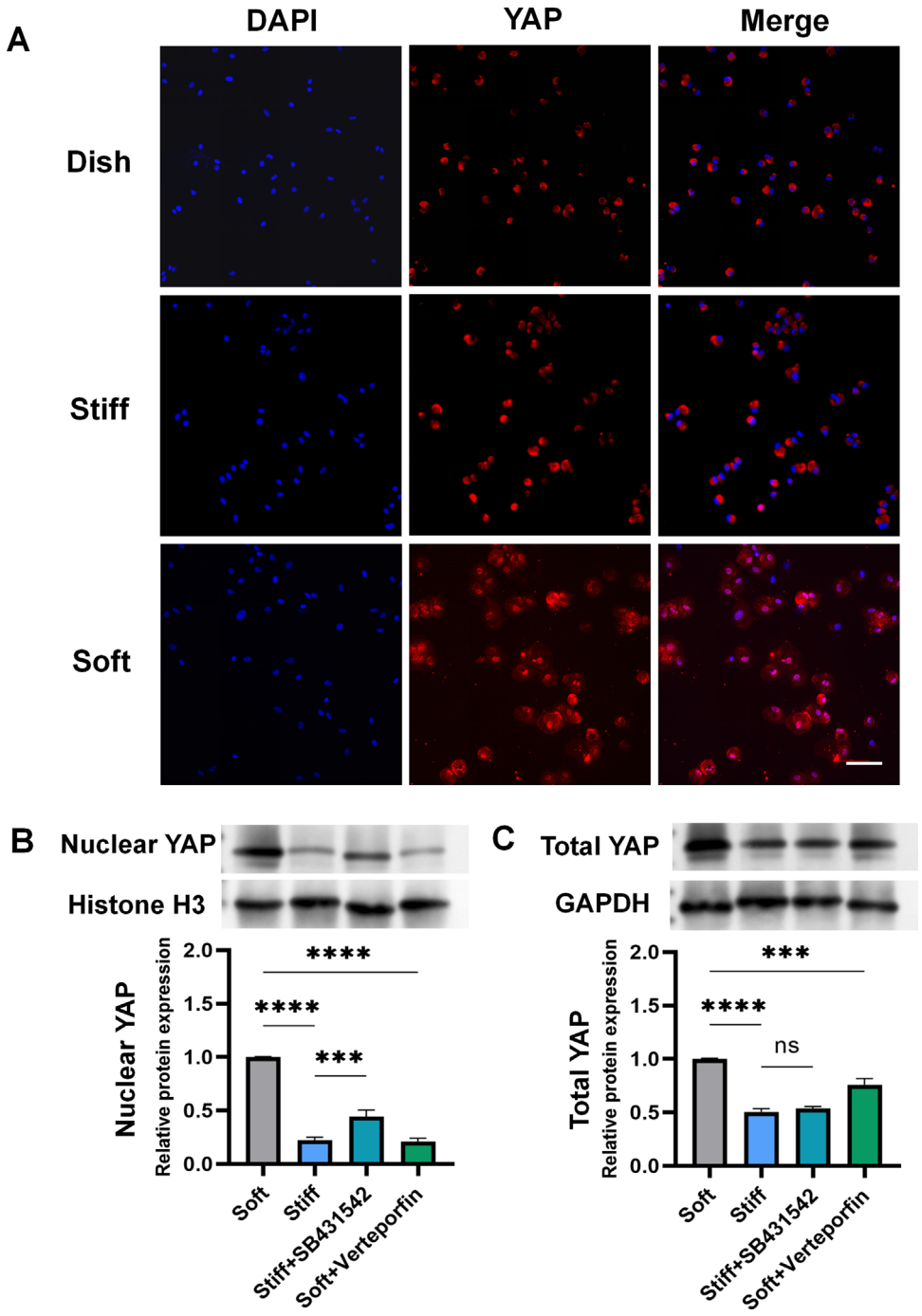

Figure 5. YAP expression on different substrates revealed distinct patterns of intracellular localization. (**A**) Immunostaining of LNC YAP on dish, stiff, and soft substrates. *Scale bar*: 200 µm. (**B**, **C**) Nuclear YAP were extracted using a nuclear and cytoplasmic extraction kit, and the expression levels of nuclear and total YAP were detected. SB431542 treatment increased nuclear YAP levels on the stiff substrate, whereas verteporfin successfully inhibited nYAP. All quantitative data are presented as mean ± SD. ****$P < 0.0001$, ***$P < 0.001$.

tive levels of α-SMA and S100A4 were lower in the group representing the stiffness of limbus. Moreover, COL1A1, which is indicative of abnormal precipitation of the extracellular matrix, also varied significantly in positive levels among the groups. This finding suggests that stiffness, mostly caused by fibrosis of the initial injury, inevitably affects the function of the support cells and the composition of the niche materials in the limbal niche continuously even after the injury has healed and will further affect the function and state of the adult stem cells it contains.[33] A significant advancement in understanding tissue repair and the pathogenesis of fibrosis is the recognition that the biophysical properties of tissues undergoing repair, particularly increased matrix stiffness, can engage in a positive feedback loop with myofibroblast activation and persistence.[36,37] Within this loop, heightened matrix stiffness facilitates myofibroblast differentiation and activation. The subsequent augmented deposition and cross-linking

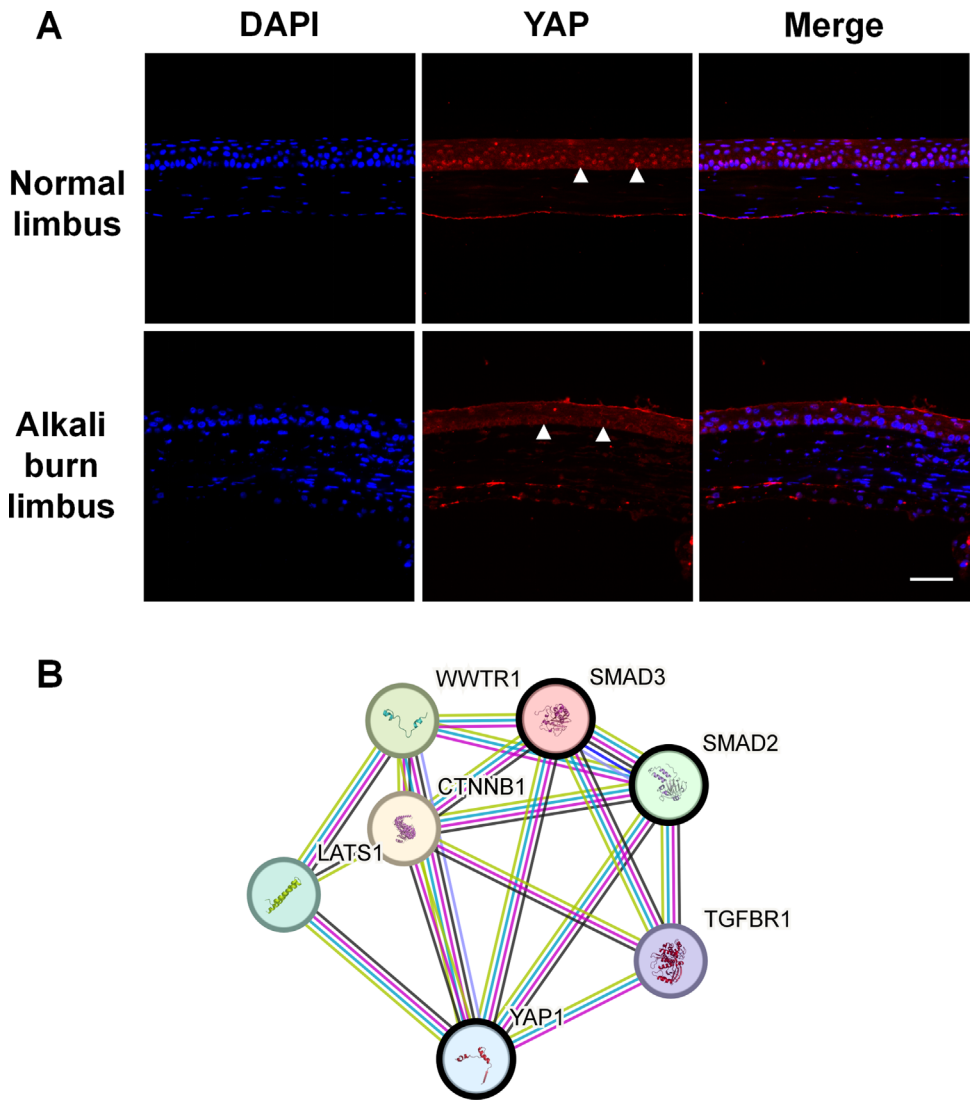

Figure 6. YAP expression in normal and alkali-burn mouse limbus. (**A**) YAP was located in the nucleus of normal mouse limbal cells, but in the alkali-burned limbus YAP lost its nuclear expression. *Scale bar*: 100 µm. (**B**) YAP-related protein interaction map shows that YAP interacted closely with SMAD2 and SMAD3 protein.

of ECM proteins by these activated myofibroblasts further enhance matrix stiffness, thereby perpetuating the amplification loop.[36]

Classically, the specific physical factors contained in the stem cell niche, such as matrix stiffness, play an important role in regulating stem cell morphological structure (e.g., adhesion, spreading) and function (e.g., proliferation, differentiation).[38] In most cases, in response to stiff matrix signals, YAP translocates from the cytoplasm to the nucleus and promotes stem cell proliferation and a differentiated phenotype.[10,16,38,39] In this study, those in the stiff group showed higher abnormal cYAP levels, which is not consistent with many studies linking nYAP to stiffer substrates. However, other recent studies have reported that lower stiffness can instead increase the proportion of nYAP in stem cells. Bhattacharya et al.[20] proposed that the reason may be that the stiffness of cornea relative to other tissues stimulates another signaling pathway, the SMAD2/3 signaling pathway, and ultimately leads to cYAP localization.

Our subsequent detection of the SMAD2/3 pathway confirmed that this theory is also valid for LNCs. Posphorylated SMAD2/3 in the stiff substrate culture system prevented YAP from entering the nucleus and initiated the myofibrotic process of LNCs via the SMAD/α-SMA axis, which can be blocked by SMAD inhibitor. Consistent with previous literature reporting that inhibiting TGF-β signaling can promote stem cell pluripotency,[40,41] successful nuclear translocation of YAP in the soft substrate enables subsequent expression of embryonic stem cell markers such as OCT4 and SOX2.[42,43] YAP is a transcriptional coactivator protein that has been widely studied as a downstream effector of Hippo signaling pathway, and it is expressed in various tissues of human body. Hippo/YAP signal transduction plays an important role in organ size regulation, cancer occurrence, tissue regeneration, and stem cell function and regulates tissue growth and organ size by positively regulating the proliferate activity of stem cells and progenitor cells.[44] Independent of the Hippo pathway, YAP can also respond to mechanical signals inside and outside the cell to regu-

Investigative Ophthalmology & Visual Science

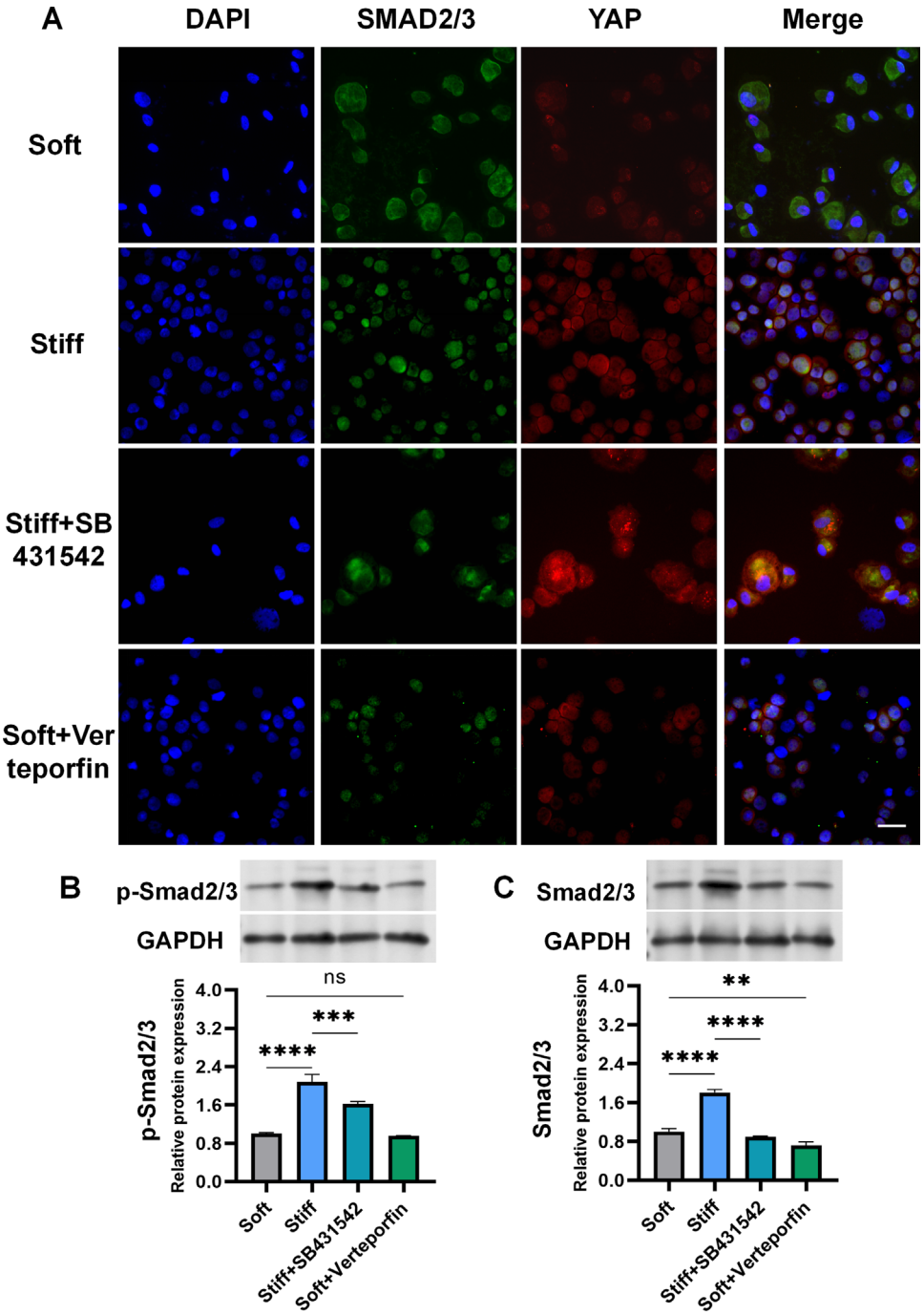

Figure 7. Blocking YAP and SMAD signaling in LNCs suggests their roles. (**A**) The stiff substrate stimulated SMAD2/3 to enter the nucleus and YAP was distributed in the cytoplasm, but the situation was reversed on the soft substrate. The application of the SMAD inhibitor SB431542 effectively blocked SMAD2/3 activity within the nucleus and partially reinstated the nuclear expression of YAP. Use of the YAP inhibitor verteporfin verified the roles of YAP and SMAD2/3. *Scale bar*: 100 µm. (**B**, **C**) Western blot was used to detect the levels of p-Smad2/3 and Smad2/3 separately. Compared with the soft group, significantly higher levels of activated p-Smad and Smad2/3 were observed in the stiff group. After treatment with the dual SMAD inhibitor SB431542, the expression of both p-SMAD2/3 and SMAD2/3 was reduced. All quantitative data are presented as mean ± SD. $^{****}P < 0.0001$, $^{***}P < 0.001$, $^{**}P < 0.01$.

late cell function and tissue homeostasis. Additionally, YAP, along with transcriptional co-activator with PDZ-binding motif (TAZ), has been identified as a mechanoregulator of TGF-β/SMAD signaling, which is crucial for renal fibrogenesis. The stiffening of the kidney after injury is recognized as a significant driver of fibrogenesis, and YAP/TAZ proteins are mechanosensory elements that bind to SMAD transcription factors, mediating profibrotic responses.[26] In many cases, in response to stiff matrix signals, YAP translocates from the cytoplasm to the nucleus and promotes cell proliferation and differentiation. The role of YAP in maintaining the pluripotency of stem cells, especially MSCs, has been explored in

Investigative Ophthalmology & Visual Science

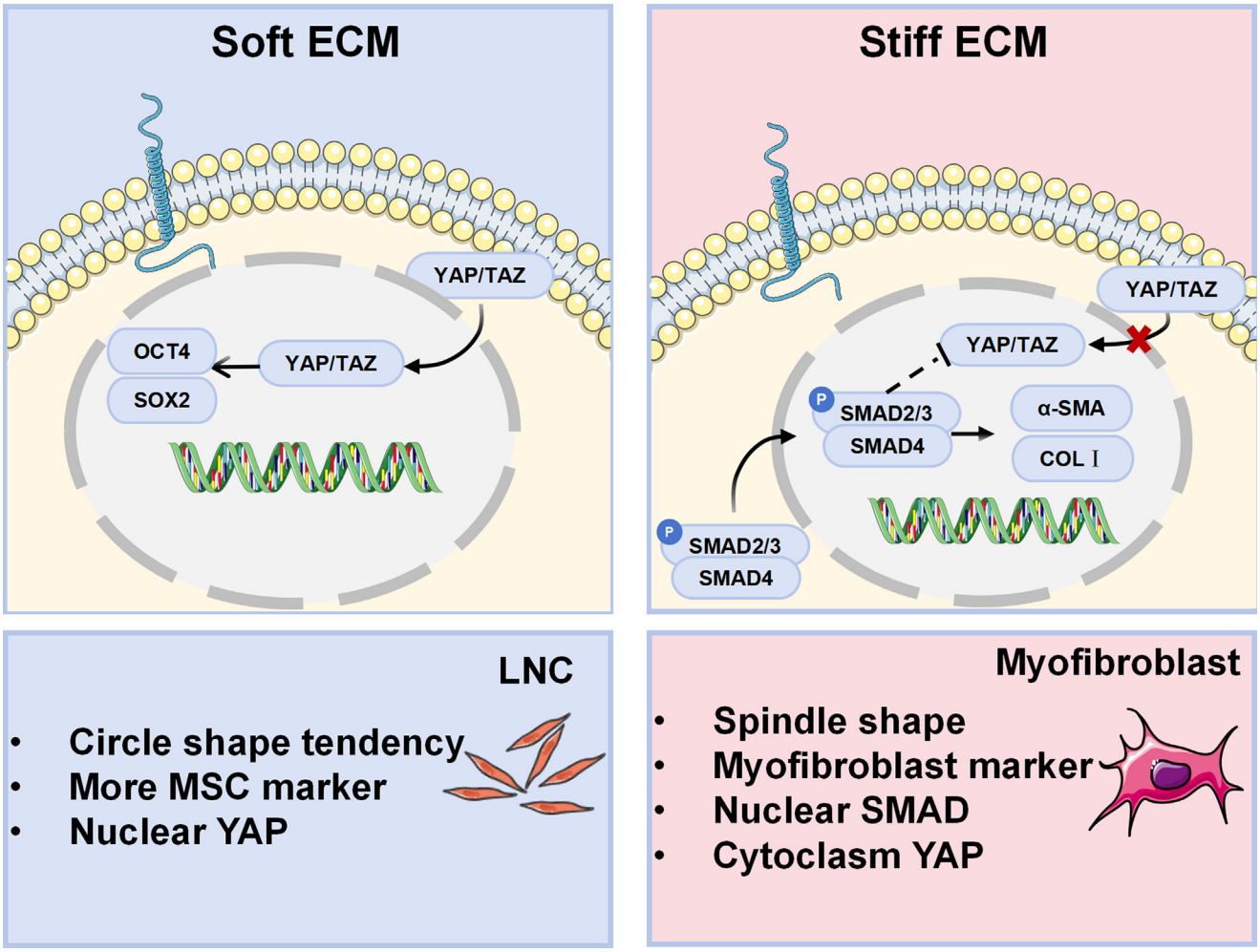

Figure 8. An illustration of how matrix stiffness influenced the behavior of LNCs through mechanotransduction. In soft ECM, YAP entered the nucleus and activated downstream signaling molecules to maintain the morphology and stem cell characteristics of the LNCs. However, when the ECM stiffness increased, the nuclear expression of SMAD2/3 proteins inhibited the nuclear translocation of YAP, leading to differentiation of LNC cells toward myofibroblast.

some studies.[44–47] Especially in the limbal niche, the role of YAP in maintaining the undifferentiated state of stem cells has been highlighted.[20] Interestingly, by removing collagen in the corneal limbus following alkali burn, Gouveia et al.[10] successfully recovered the limbal natural LSC-supporting capacity.

Conclusions

In this study, we explored the influence of substrate stiffness on LNCs by constructing culture systems with substrates of varying stiffness to reveal their morphology, stem cell characteristics, and the key trigger pathway of fibroblast transformation. Specifically, the loss of stem cell phenotype and myofibrosis occurred in stiff LNCs but not in soft LNCs. These changes were accompanied by an altered nYAP/cYAP ratio. We found that corneal stiffness and even greater stiffness of the substrates stimulated SMAD2/3 to enter the nucleus, which inhibited the nuclear translocation of YAP and triggered the subsequent myofibrogenesis process. In contrast, soft substrates promoted nYAP conversion by limiting SMAD2/3, and the YAP/SOX2/OCT4 axis was thus delivered. In conclusion, this study provides new insights into the response of different tissue-derived cells to YAP and offers a new perspective for the treatment of some fibrosis-related diseases.

Acknowledgments

Supported by grants from the National Natural Science Foundation of China (82471050, 82070936), the Ministry of Science and Technology of China (S20240235), and the Science and Technology Talent Service Enterprise Project of Department of Science and Technology of Hubei Province (2024DJC066).

Disclosure: **X. Zhou**, None; **L. Xu**, None; **Y. Tan**, None; **W. Wang**, None; **X. Huang**, None; **G. Li**, None

References

1. Li W, Hayashida Y, Chen YT, Tseng SC. Niche regulation of corneal epithelial stem cells at the limbus. *Cell Res*. 2007;17:26–36.
2. Dimmock R, Zhang Y, Butt GF, Rauz S, Huang Z, Yang Y. Characterizing biomechanics of limbal niche using vibrational optical coherence elastography. *J Biophotonics*. 2024;17:e202400172.

3. Moreno IY, Parsaie A, Gesteira TF, Coulson-Thomas VJ. Characterization of the limbal epithelial stem cell niche. *Invest Ophthalmol Vis Sci*. 2023;64:48.
4. Xie HT, Chen SY, Li GG, Tseng SC. Isolation and expansion of human limbal stromal niche cells. *Invest Ophthalmol Vis Sci*. 2012;53:279–286.
5. Su G, Guo X, Xu L, et al. Isolation and characterization of rabbit limbal niche cells. *Exp Eye Res*. 2024;241:109838.
6. Zhu H, Wang W, Tan Y, et al. Limbal niche cells and three-dimensional matrigel-induced dedifferentiation of mature corneal epithelial cells. *Invest Ophthalmol Vis Sci*. 2022;63:1.
7. Jin B, Su G, Zhou X, et al. Basic fibroblast growth factor supports the function of limbal niche cells via the Wnt/β-catenin pathway. *J Ocul Pharmacol Ther*. 2024;40:571–580.
8. Li GG, Chen SY, Xie HT, Zhu YT, Tseng SC. Angiogenesis potential of human limbal stromal niche cells. *Invest Ophthalmol Vis Sci*. 2012;53:3357–3367.
9. Lepert G, Gouveia RM, Connon CJ, Paterson C. Assessing corneal biomechanics with Brillouin spectro-microscopy. *Faraday Discuss*. 2016;187:415–428.
10. Gouveia RM, Lepert G, Gupta S, Mohan RR, Paterson C, Connon CJ. Assessment of corneal substrate biomechanics and its effect on epithelial stem cell maintenance and differentiation. *Nat Commun*. 2019;10:1496.
11. Yagi R, Chen LF, Shigesada K, Murakami Y, Ito Y. A WW domain-containing yes-associated protein (YAP) is a novel transcriptional co-activator. *EMBO J*. 1999;18:2551–2562.
12. Engler AJ, Sen S, Sweeney HL, Discher DE. Matrix elasticity directs stem cell lineage specification. *Cell*. 2006;126:677–689.
13. Dupont S, Morsut L, Aragona M, et al. Role of YAP/TAZ in mechanotransduction. *Nature*. 2011;474:179–183.
14. Panciera T, Azzolin L, Cordenonsi M, Piccolo S. Mechanobiology of YAP and TAZ in physiology and disease. *Nat Rev Mol Cell Biol*. 2017;18:758–770.
15. Gouveia RM, Vajda F, Wibowo JA, Figueiredo F, Connon CJ. YAP, ΔNp63, and β-catenin signaling pathways are involved in the modulation of corneal epithelial stem cell phenotype induced by substrate stiffness. *Cells*. 2019;8:347.
16. Zhang X, Cao D, Xu L, et al. Harnessing matrix stiffness to engineer a bone marrow niche for hematopoietic stem cell rejuvenation. *Cell Stem Cell*. 2023;30:378–395.e8.
17. Liu S, Chen H, Xie H, Liu X, Zhang M. Substrate stiffness modulates stemness and differentiation of rabbit corneal endothelium through the paxillin-YAP pathway. *Invest Ophthalmol Vis Sci*. 2024;65:15.
18. Caliari SR, Vega SL, Kwon M, Soulas EM, Burdick JA. Dimensionality and spreading influence MSC YAP/TAZ signaling in hydrogel environments. *Biomaterials*. 2016;103:314–323.
19. Brusatin G, Panciera T, Gandin A, Citron A, Piccolo S. Biomaterials and engineered microenvironments to control YAP/TAZ-dependent cell behaviour. *Nat Mater*. 2018;17:1063–1075.
20. Bhattacharya S, Mukherjee A, Pisano S, et al. The biophysical property of the limbal niche maintains stemness through YAP. *Cell Death Differ*. 2023;30:1601–1614.
21. Li Y, Ge L, Chen X, et al. The common YAP activation mediates corneal epithelial regeneration and repair with different-sized wounds. *NPJ Regen Med*. 2021;6:16.
22. Foster JW, Jones RR, Bippes CA, Gouveia RM, Connon CJ. Differential nuclear expression of Yap in basal epithelial cells across the cornea and substrates of differing stiffness. *Exp Eye Res*. 2014;127:37–41.
23. Massague J. TGF-β signal transduction. *Annu Rev Biochem*. 1998;67:753–791.
24. Mou H, Vinarsky V, Tata PR, et al. Dual SMAD signaling inhibition enables long-term expansion of diverse epithelial basal cells. *Cell Stem Cell*. 2016;19:217–231.
25. Grannas K, Arngarden L, Lonn P, et al. Crosstalk between Hippo and TGFβ: subcellular localization of YAP/TAZ/Smad complexes. *J Mol Biol*. 2015;427:3407–3415.
26. Szeto SG, Narimatsu M, Lu M, et al. YAP/TAZ are mechanoregulators of TGF-β-Smad signaling and renal fibrogenesis. *J Am Soc Nephrol*. 2016;27:3117–3128.
27. Thomasy SM, Raghunathan VK, Winkler M, et al. Elastic modulus and collagen organization of the rabbit cornea: epithelium to endothelium. *Acta Biomater*. 2014;10:785–791.
28. Su G, Wang W, Xu L, et al. Isolation and identification of limbal niche cells. *J Vis Exp*. 2023;200:e65618.
29. Sprogyte L, Park M, Nureen L, Tedla N, Richardson A, Di Girolamo N. Development and characterization of a preclinical mouse model of alkali-induced limbal stem cell deficiency. *Ocul Surf*. 2024;34:329–340.
30. Eberwein P, Nohava J, Schlunck G, Swain M. Nanoindentation derived mechanical properties of the corneascleral rim of the human eye. *Biophys J*. 2014;106:789A.
31. Yazdanpanah G, Haq Z, Kang K, Jabbehdari S, Rosenblatt ML, Djalilian AR. Strategies for reconstructing the limbal stem cell niche. *Ocul Surf*. 2019;17:230–240.
32. Di Girolamo N. Biologicals and biomaterials for corneal regeneration and vision restoration in limbal stem cell deficiency. *Adv Mater*. 2024;36:e2401763.
33. Nowell CS, Odermatt PD, Azzolin L, et al. Chronic inflammation imposes aberrant cell fate in regenerating epithelia through mechanotransduction. *Nat Cell Biol*. 2016;18:168–180.
34. Koester J, Miroshnikova YA, Ghatak S, et al. Niche stiffening compromises hair follicle stem cell potential during ageing by reducing bivalent promoter accessibility. *Nat Cell Biol*. 2021;23:771–781.
35. Segel M, Neumann B, Hill MFE, et al. Niche stiffness underlies the ageing of central nervous system progenitor cells. *Nature*. 2019;573:130–134.
36. Liu F, Mih JD, Shea BS, et al. Feedback amplification of fibrosis through matrix stiffening and COX-2 suppression. *J Cell Biol*. 2010;190:693–706.
37. Parker MW, Rossi D, Peterson M, et al. Fibrotic extracellular matrix activates a profibrotic positive feedback loop. *J Clin Invest*. 2014;124:1622–1635.
38. Li JJ, Liu YF, Zhang YJ, et al. Biophysical and biochemical cues of biomaterials guide mesenchymal stem cell behaviors. *Front Cell Dev Biol*. 2021;9:640388.
39. Sheng R, Liu J, Zhang W, et al. Material stiffness in cooperation with macrophage paracrine signals determines the tenogenic differentiation of mesenchymal stem cells. *Adv Sci (Weinh)*. 2023;10:e2206814.
40. Hassani SN, Totonchi M, Sharifi-Zarchi A, et al. Inhibition of TGFβ signaling promotes ground state pluripotency. *Stem Cell Rev Rep*. 2014;10:16–30.
41. Tan F, Qian C, Tang K, Abd-Allah SM, Jing N. Inhibition of transforming growth factor β (TGF-β) signaling can substitute for Oct4 protein in reprogramming and maintain pluripotency. *J Biol Chem*. 2015;290:4500–4511.
42. Seo E, Basu-Roy U, Gunaratne PH, et al. SOX2 regulates YAP1 to maintain stemness and determine cell fate in the osteo-adipo lineage. *Cell Rep*. 2013;3:2075–2087.
43. Bora-Singhal N, Nguyen J, Schaal C, et al. YAP1 regulates OCT4 activity and SOX2 expression to facilitate self-renewal and vascular mimicry of stem-like cells. *Stem Cells*. 2015;33:1705–1718.

Investigative Ophthalmology & Visual Science

44. Camargo FD, Gokhale S, Johnnidis JB, et al. YAP1 increases organ size and expands undifferentiated progenitor cells. *Curr Biol*. 2007;17:2054–2060.
45. Lian I, Kim J, Okazawa H, et al. The role of YAP transcription coactivator in regulating stem cell self-renewal and differentiation. *Genes Dev*. 2010;24:1106–1118.
46. Fu L, Hu Y, Song M, et al. Up-regulation of FOXD1 by YAP alleviates senescence and osteoarthritis. *PLoS Biol*. 2019;17:e3000201.
47. Cao X, Pfaff SL, Gage FH. YAP regulates neural progenitor cell number via the TEA domain transcription factor. *Genes Dev*. 2008;22:3320–3334.

Investigative Ophthalmology & Visual Science